P9.30

ESTIMATING THE REFRACTIVE INDEX STRUCTURE-FUNCTION AND RELATED OPTICAL SEEING PARAMETERS WITH THE WRF-ARW

Eric M. Kemp,* Billy D. Felton, and Randall J. Alliss
Northrop Grumman Information Technology/TASC, Chantilly, Virginia

1. INTRODUCTION

Atmospheric turbulence can significantly degrade the quality of optical communications systems. It is therefore essential to characterize expected turbulence before using such a system. Unfortunately it can be very difficult and expensive to instrument regions for measuring relevant atmospheric conditions. A more economical alternative is to employ numerical weather prediction to estimate turbulence climatology.

The key variable of interest is the refractive index structure-function parameter (C_n^2). When turbulence is locally homogeneous and isotropic, C_n^2 is related to changes in the refractive index δn over distance r (Tatarskii 1971):

$$\overline{(\delta n)^2} = C_n^2 r^{2/3}$$

where the overbar indicates an ensemble average, and r lies within the inertial subrange of turbulence. Larger values of C_n^2 correspond to increasing changes in the refractive index. Closely related is the *Fried parameter* (r_0):

$$r_0 = \left[0.423\left(\frac{2\pi}{\lambda}\right)^2 \int_0^\infty C_n^2(z)dz\right]^{-3/5}$$

where λ is the optical wavelength. Fried (1965) introduced r_0 to measure the magnitude of the phase distortion of an optical wavefront by turbulence. Smaller values of r_0 indicate more severe turbulence, and increasingly degraded *atmospheric seeing* conditions.

In this paper we describe using the WRF-ARW to estimate seeing climatologies over different geographical areas in the United States. Our work is complementary to that of Cherubini et al. (2008) and of Masciadri and coworkers (Masciadri and Enger 2006; Masciadri and Jabouille 2001; Masciadri et al. 2001). Section 2 describes the model configuration, modifications to the WRF Mellor-Yamada-Janjić (MYJ) turbulence closure, and calculation of seeing parameters. Example results for a region in New Mexico are given in section 3. Section 4 provides a summary and discusses future work.

2. TECHNIQUE

a. Domain Configuration

We have used WRF-ARW Version 2.2 to simulate daily weather conditions at several locations in the United States for 2006–2007. In each case the model is configured at 1-km horizontal resolution with dimensions 67×63. The number of vertical grid points varies from 135 to 140, with the sigma levels set to approximate 50 m resolution below 2 km above ground level (AGL), 125 m for 2-12 km AGL, and 500 m up to 50 mb. (These exact resolutions would require flat terrain and conditions matching the U.S. Standard Atmosphere.) Simulations are initialized at 1200 UTC directly from the 12-km (Grid 218) North American Mesoscale (NAM) analysis produced by the National Weather Service. Lateral boundary conditions are provided out to 27 hours by three-hourly NAM forecasts. This allows us to to filter out model "spin-up" by excluding the first 3 simulation hours from our studies, while still capturing the full 24-hour diurnal cycle. Selected physics and diffusion options are summarized in Table 1.

b. Modifications to WRF

We found it necessary to modify the minimum turbulence kinetic energy (TKE) permitted in the MYJ scheme. The default setting of parameter **epsq2** in MODULE_MODEL_CONSTANTS.F gives TKE values $\geq$ 0.01 m^2 s^{-2}, resulting in unrealistically large values of C_n^2 in the free atmosphere. Following Gerrity et al. (1994), we changed the minimum TKE limit to 0.00001 m^2 s^{-2}.

The second modification involves the eddy diffusivities of heat and momentum (K_H and K_M, respectively). In the original MYJ scheme, these vari-

**Corresponding author address*: Eric M. Kemp, Northrop Grumman Information Technology/TASC, 4801 Stonecroft Blvd, Chantilly, VA 20151. E-mail: eric.kemp@ngc.com

Table 1: WRF physics and diffusion settings.

Time integration	RK3
Time step	2 sec
Horizontal advection	Fifth order
Vertical advection	Third order
Explicit diffusion	Physical space 2D Deformation No sixth-order
Boundary layer	MYJ
Surface layer	Janjić Eta
Land surface	Noah
Shortwave radiation	Dudhia
Longwave radiation	RRTM
Microphysics	WSM6
Cumulus parameterization	None

ables are given by:

$$K_H = \ell q S_H, K_H = \ell q S_M,$$

where ℓ is the mixing length, $q = \sqrt{2\text{TKE}}$, and S_H and S_M are functions of TKE, mixing length, buoyancy and vertical wind shear (Mellor and Yamada 1982). In our modified version we keep these relations unchanged for neutral and unstable conditions. However, when the gradient Richardson number (Ri) $>$ 0.01 we follow Walters and Miller (1999) and adjust K_M so that:

$$\frac{K_H}{K_M} = \begin{cases} \frac{1}{7Ri}, & \text{for Ri} \geq 1, \\ \frac{1}{6.873Ri + \frac{1}{1+6.873Ri}} & 0.01 < \text{Ri} \leq 1. \end{cases}$$

This equation for K_H/K_M was first proposed by Kondo et al. (1978). The Kondo equation decreases K_H/K_M with increasing Ri, effectively increasing TKE production by vertical wind shear. Walters and Miller (1999) found this necessary to generate free atmosphere turbulence associated with jet streaks, and we employ this change in all simulations.

c. *Estimating Seeing*

Tatarskii (1971) derived an alternative expression for the structure-function parameter applicable for optical wavelengths:

$$C_n^2 = \left(\frac{79 \times 10^{-8} P}{T^2}\right)^2 C_T^2$$

where P is atmospheric pressure (Pa), T is air temperature (K), and C_T^2 is the structure-function parameter for temperature. C_T^2 in turn is related to:

$$C_T^2 = a^2 \left(\frac{K_H}{K_M}\right) L_o^{4/3} \left(\frac{\partial\theta}{\partial z}\right)^2$$

where a^2 is an empirical constant, L_o is the outer length scale of turbulence (i.e., the upper bound of the inertial subrange), and $\partial\theta/\partial z$ is the vertical gradient of potential temperature. Following Walters and Miller (1999), we set a^2 to 2.8 and calculate L_o in thermally stable conditions using an approximation from Deardorff (1980):

$$L_o = 0.76\sqrt{TKE}/N$$

where N is the Brunt-Väisälä frequency. In thermally unstable conditions, L_o is related to the depth of the unstable layer, similar to Masciadri et al. (2001). With these input variables, we then calculate C_n^2 in 3D and r_0 in 2D.

3. PRELIMINARY RESULTS

A sample springtime climatology of r_0 from WRF is shown in Figure 1. For comparison, we also show observed climatological information measured from a differential image motion monitor (DIMM). The comparison shows general success in simulating the diurnal cycle of r_0 with WRF. Figure 2 shows the cumulative distribution functions (CDFs) of both datasets for the daytime. It is apparent that WRF does not produce the very lowest values of r_0 during the day–perhaps due to inadequate grid resolution. Figure 3 shows the corresponding CDF plots for nighttime. Here, WRF (in blue) shows lower r_0 values at night that are not measured by the DIMM. One partial explanation is that the DIMM was shut down whenever surface winds exceeded 30 mph. Better agreement is reached when WRF cases exceeding this wind threshold are thrown out (in green).

4. SUMMARY AND FUTURE WORK

We have generated daily simulations of atmospheric conditions for several locations with WRF, in an attempt to characterize the distribution of C_n^2 and related optical turbulence parameters. Comparisons with observations suggest some skill in capturing optical turbulence, but discrepancies are also noted. Future work will include:

- additional comparisons with observed data;
- increasing the resolution of the model domains (we are attempting to run WRF version 3.0 at 0.5 km resolution at the time of this writing);
- improving the model initialization (e.g., with 3DVAR); and
- testing other physics packages to more accurately simulate turbulence.

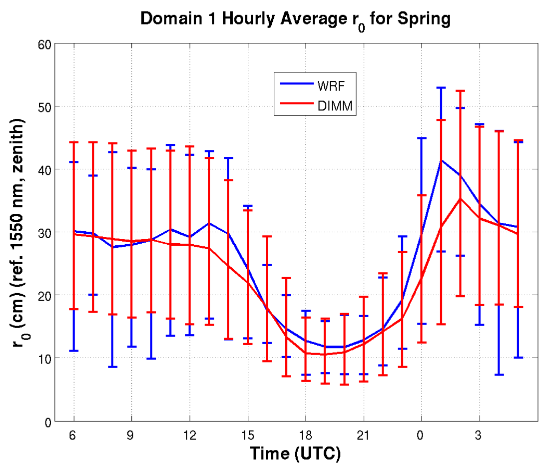

Figure 1: Diurnal cycle of r_0 from WRF and DIMM.

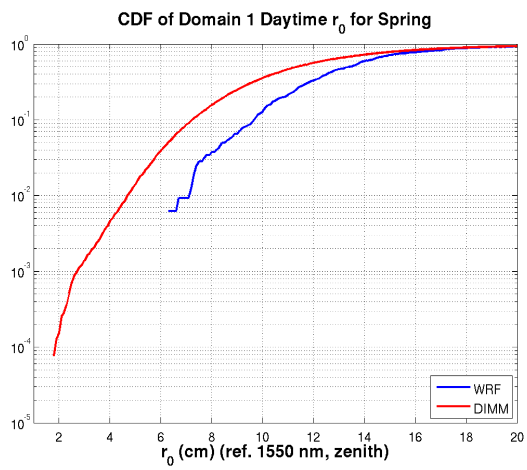

Figure 2: CDFs of daytime r_0 from WRF and DIMM.

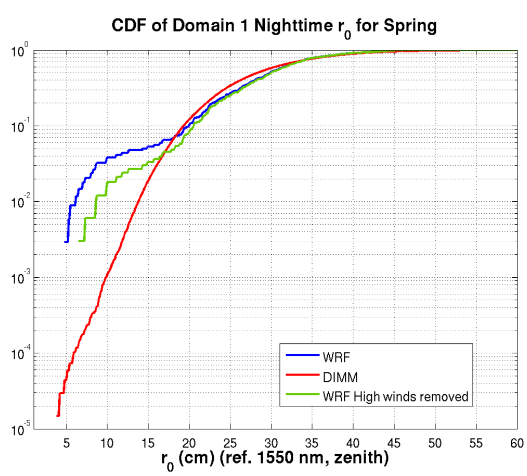

Figure 3: CDFs of nighttime r_0 from WRF and DIMM. Green curve excludes WRF cases with 30+ mph surface winds.

Acknowledgements. We thank the NGIT/TASC High Performance Computing project for making their computer resources available. We particularly thank Joe Greenseid and Robert Link for their system administration support. Archived NAM GRIB data was provided by the National Climatic Data Center via the National Operational Model Archive and Distribution System (http://nomads.ncdc.noaa.gov/).

References

Cherubini, T., S. Businger, R. Lyman, and M. Chun, 2008: Modeling optical turbulence and seeing over Mauna Kea. *J. Appl. Meteor. Climatol.*, **47**, 1140–1155.

Deardorff, J. W., 1980: Stratocumulus-capped mixed layers derived from a three-dimenstional model. *Bound.-Layer Meteor.*, **18**, 495–527.

Fried, D. L., 1965: Statistics of a geometric representation of wavefront distortion. *J. Opt. Soc. Amer.*, **55**, 1427–1435.

Gerrity, J. P., T. L. Black, and R. E. Treadon, 1994: The numerical solution of the Mellor-Yamada level 2.5 turbulent kinetic energy equation in the Eta model. *Mon. Wea. Rev.*, **122**, 1640–1646.

Kondo, J., O. Kanechika, and N. Yasuda, 1978: Heat and momentum transfers under strong stability in the atmospheric surface layer. *J. Atmos. Sci.*, **35**, 1012–1021.

Masciadri, E. and S. Enger, 2006: First seasonal study of optical turbulence with an atmospheric model. *Pub. Astron. Soc. Pac.*, **118**, 1604–1619.

Masciadri, E. and P. Jabouille, 2001: Improvements in the optical turbulence parameterization for 3D simulations in a region around a telescope. *Astron. Astrophys.*, **376**, 727–734.

Masciadri, E., J. Vernin, and P. Bougeault, 2001: 3D numerical simulations of optical turbulence at the Roque de Los Muchachos Observatory using the atmospheric model Meso-NH. *Astron. Astrophys.*, **365**, 699–708.

Mellor, G. L. and T. Yamada, 1982: Development of a turbulence closure model for geophysical fluid problems. *Rev. Geophys. Space Phys.*, **20**, 851–875.

Tatarskii, V. I., 1971: The effects of the turbulent atmosphere on wave propagation. Technical report, U.S. Department of Commerce, NTIS TT-68-50464. 472pp.

Walters, D. L. and D. K. Miller, 1999: Evolution of an upper-tropospheric turbulence event–Comparison of observations to numerical simulations. *Preprints, 13th Symposium on Boundary Layer Turbulence*, AMS, 157–160, Dallas, TX.